STM JOURNALS

Journal of
Polymer & Composites

ISSN: 2321-2810 (Online)
ISSN: 2321-8525 (Print)
Volume 14, Special Issue 3, 2026
DOI (Journal): 10.37591/JoPC

https://journals.stmjournals.com/jopc

Research JoPC

Polymer-Mediated Electron Transfer in Eco-Friendly P3HT–rGO Nanocomposites for Optoelectronic Applications

Sumit Kumar[1*], Tanvi Vats[2], Ashu Soni[3] and Pratibha Tiwari[4]

Abstract

Conducting polymer–graphene hybrid nanocomposites have emerged as promising materials for next-generation optoelectronic applications owing to their solution processability, tunable interfacial properties, and mechanical flexibility. Recent studies have highlighted the importance of graphene–polymer hybrid systems in enhancing charge transport pathways, exciton dissociation efficiency, and interfacial stability in organic optoelectronic devices. Despite these advantages, a key challenge remains the efficient production of individual graphene sheets through the reduction of graphene oxide using inexpensive, scalable, and solution-processable techniques that are compatible with sustainable and environmentally benign processing. In this work, an eco-friendly, single-step chemical reduction strategy is employed to reduce graphene oxide using L-glutathione (GSH) as a green reducing agent, targeting optoelectronic applications such as organic photovoltaics. Nanocomposites of green-route reduced graphene oxide (rGO) are blended with conducting regioregular poly(3-hexylthiophene) (P3HT) to investigate polymer-mediated electron transfer processes and interfacial interactions. The reduction of graphene oxide and its dispersion within the polymer matrix are characterized using Fourier transform infrared spectroscopy (FTIR), X-ray diffraction (XRD), scanning electron microscopy (SEM), and atomic force microscopy (AFM). Electron transfer behavior in the nanocomposites is examined using UV–Vis absorption and photoluminescence (PL) spectroscopy. The observed photoluminescence quenching indicates efficient exciton dissociation and suppressed radiative recombination in rGO–P3HT blends, confirming enhanced excited-state electron transfer at the polymer–rGO interface and highlighting the potential of eco-friendly polymer–graphene nanocomposites for sustainable optoelectronic applications.

***Author for Correspondence**
Sumit Kumar

[1]Professor, Department of Electronics and Communication Engineering, Faculty of Engineering and Technology, JAIN (Deemed-to-be University) Bangalore, Karnataka, India
[2]Assistant Professor, Department of Applied Chemistry, Gautam Buddha University, Yamuna Expressway, Greater Noida, Uttar Pradesh, India
[3]Assistant Professor, Department of Electronics and Communication Engineering, Bharati Vidyapeeth College of Engineering, New Delhi, India
[4]Associate Professor, Department of Chemistry, Hansraj College, University of Delhi, New Delhi, India

Received Date: March 14, 2026
Accepted Date: April 30, 2026
Published Date: May 16, 2026

Citation: Sumit Kumar, Tanvi Vats, Ashu Soni and Pratibha Tiwari. Polymer-Mediated Electron Transfer in Eco-Friendly P3HT–rGO Nanocomposites for Optoelectronic Applications. Journal of Polymer & Composites. 2026; 14(Special Issue 3): S413–S423p.

Keywords: Reduced graphene oxide (rGO), P3HT polymer, nanocomposites, organic solar cells, electron transfer

INTRODUCTION

Lightweight nature, increased utility due to flexibility, lower processing expenses and greater environmental sustainability has sphereheaded organic solar cells as a non-conventional energy source [1–3]. Among the main advantages of organic solar cells, the most important is their ease of processing and device fabrication, particularly those based on conducting polymers. The active layers can be deposited through solution-based methods, which mainly comprise of spin coating and printing. These methods result in device fabrication at lower temperatures and thus are

highly cost effective. The working mechanism of these devices is governed by exciton generation within the polymer donor phase, followed by electron-hole separation at donor–acceptor interfaces.

Organic solar cells have gained significant attention as promising alternatives to conventional silicon-based photovoltaic devices due to their low-cost fabrication, mechanical flexibility, and tunable optoelectronic properties. The polymer solar cells are transparent in nature and hence find a potential application as windows panes and flexible electronics. However, they come with the disadvantages such as low power conversion efficiency and photochemical degradation [4]. A commonly used conjugated polymer in polymer based solar cells and organic light emitting devices is poly(3-hexylthiophene) (P3HT). The extensively conjugated thiophene rings gave rise to π-π* transitions over a broad range of 500−900 nm. In such polymer systems, the efficiency of exciton dissociation and subsequent electron transfer is strongly governed by the interfacial interaction between the polymer donor and the acceptor material. The luminescence wavelength and bandgap of P3HT can be precisely controlled by chemically combining the conjugated system with other semiconducting materials, which facilitate exciton dissociation and migration and thereby determine the photovoltaic performance [5].

One such semiconducting material with strong potential for optoelectronics applications is graphene. Graphene exhibits excellent optical transparency, mechanical flexibility and remarkable charge transport properties [6]. Structurally, graphene is a two-dimensional (2D) material comprising of a base layer of sp^2-hybridized carbon atoms arranged in a hexagonal fashion. Graphene acts as a base for a variety of carbon-based materials, including 0D buckminsterfullerene, 1D carbon nanotubes and 3D graphite [7]. The extensive network of conjugated π-bonds equips graphene with exceptional electrical properties while strong σ bonds impart high mechanical strength [8, 9]. These properties along with the fact that graphene is the thinnest known stretchable crystal, make it a desirable material for application in optoelectronic devices, batteries, energy storage, biomaterials and biosensors [10–14]. Despite its exceptional properties, large-scale production of high-quality graphene remains challenging due to high cost, low yield, and transfer-related defects. This is attributed to the fact that top-down synthetic approaches generally yield limited quantities, and solvent introduces several defects in the final product. On the other hand, bottom-up methodologies require expensive equipment and high processing temperatures. Although the graphene obtained through these routes is high in quality, but remains low in yield [15]. In addition, transferring thin graphene layers from one substrate to another is a complex process that may lead to wrinkles, cracks, and fragmented graphene regions [16].

An alternative to pristine graphene could be graphene oxide (GO). It is easy to synthesize from graphite flakes via chemical [17], electrochemical [18] and exfoliation [19] methods, which are well studied. GO has a two-dimensional structure similar to graphene, but the carbon atoms are functionalized by oxygen-containing functional groups such as epoxy, hydroxyl, and carbonyl. These functional groups contribute to good colloidal stability as well as favorable mechanical and electrical characteristics. Fine-tuning of GO properties makes it suitable for multifunctional gels, drug delivery, water purification, membranes, cellular migration, neuronal generation, supercapacitors, solar cells, and sensor applications [20–25]. However, a major challenge associated with GO is that most synthetic methods employ strong oxidizing agents, leading to defect formation in the resulting material and thereby impacting the optoelectronic properties.

Several studies have explored the integration of conducting polymers with graphene-based materials to enhance charge transport and optoelectronic performance [6]. In particular, P3HT-based nanocomposites incorporating GO and rGO have demonstrated improved exciton dissociation and charge carrier mobility due to the formation of efficient donor–acceptor interfaces [26]. Generally spectroscopic investigations, especially photoluminescence studies have been widely employed to probe charge transfer mechanisms in such systems, where quenching behavior is often attributed to electron transfer from the polymer to graphene-based acceptors [27]. However, most reported approaches rely on chemically intensive reduction methods that may introduce structural defects or limit

compatibility with polymer matrices. Furthermore, limited attention has been given to eco-friendly reduction strategies that simultaneously ensure effective dispersion and enhanced interfacial interaction in polymer nanocomposites. These gaps highlight the need for sustainable synthesis routes and systematic investigation of polymer-mediated electron transfer mechanisms in graphene-based hybrid systems.

It is imperative to note that graphite-like characteristics can be recovered from GO through reductive treatments, converting GO to rGO [28]. Various reduction approaches have been reported, leading to rGO with differing degrees of reduction and interfacial compatibility [29–30]. In addition, multi-step combined methods have also been employed to generate rGO [31]. It is worth mentioning that variations in the reduction process result in rGO with different structural and electronic qualities, primarily determined by the degree of reduction. Taking this into consideration, a single-step chemical reduction approach was employed to reduce GO in an aqueous media under moderate conditions, using L-Glutathione (GSH) as a reducing agent [32, 33]. The importance of this reduction technique relies on the fact that the oxidized products of GSH act as a capping agent, further stabilizing rGO in aqueous as well as polar aprotic solvents such as tetrahydrofuran (THF), dimethyl sulfoxide (DMSO), dimethylformamide (DMF), ethyl acetate (EA). Due to the presence of terminal carboxylic group, sufficient negative charge and electrostatic repulsion develop within the reduced graphene oxide sheets, enhancing their stability in the aqueous media and compatible solvents [32]. However, limited attention has been given to polymer-compatible, eco-friendly reduction routes that directly influence electron transfer at polymer–rGO interfaces.

The present study addresses the critical need for eco-friendly and polymer-compatible graphene-based materials for optoelectronic applications. By employing L-glutathione as a green reducing agent, a sustainable route for the synthesis of reduced graphene oxide is demonstrated, ensuring improved dispersion and interfacial compatibility with the conducting polymer P3HT. The work further highlights the role of polymer–rGO interfacial interactions in governing exciton dissociation and charge transfer dynamics, as demonstrated through photoluminescence quenching and Stern–Volmer analysis. These findings provide valuable insights into the design of efficient, low-cost, and environmentally sustainable polymer–graphene hybrid systems for advanced optoelectronic devices.

METHODOLOGY

The nanocomposites are prepared using a simple solution processing technique in which the ratio between the conducting polymer donor (P3HT) and the acceptor semiconductor is estimated for forming an efficient bulk heterojunction system. Here, GO powder was obtained from Sigma Aldrich and dispersed in deionized water (DI) water. The GO solution (0.1 mg mL^{-1}) was prepared with 20 ml of DI water and initially ultrasonically bathed for 60 minutes. This ultrasonication treatment leads to additional exfoliation of GO sheets, resulting in a stable brown-colored dispersion of GO sheets in DI water. Further, GO sheets mixed with L-GSH (2.0 $mgmL^{-1}$) were ultrasonically processed for an additional hour, followed by chemical reduction to obtain polymer-compatible rGO. The mixture was then kept at 60 °C for 10 h while being vigorous stirring, cooled to room temperature, and the suspended rGO sheets were carefully separated and repeatedly washed with DI water. Finally, a stable rGO nanosheet dispersion was obtained in aqueous media. Subsequently, nanocomposites of rGO(GSH) and conducting polymer P3HT were dispersed in chloroform and THF with different compositions to investigate polymer-mediated structural, morphological, and optical properties, including absorption and emission characteristics. This work primarily focused on the investigation of the active-layer-like interaction between rGO and P3HT, which are indicative of exciton separation at donor-acceptor interfaces and effective excited electron-state electron transfer. Photoluminescence (PL) quenching studies were carried out to examine this behavior, while structural and morphological validation was achieved through the combined use of complementary analytical techniques. The analysis primarily emphasizes spectroscopic indicators of electron-transfer efficiency, relevant for evaluating the suitability of the polymer–rGO system for optoelectronic applications.

RESULTS AND DISCUSSIONS

Several characterization tools and techniques have been used in this work to establish the formation of rGO as well as synthesis of conducting polymer–based (rGO-P3HT) nanocomposites. These include X-Ray Diffraction (XRD), scanning electron microscopy (SEM), atomic force microscopy (AFM), and Fourier transform infrared (FTIR) spectroscopy. Optical techniques, including UV-vis absorption and photoluminescence (PL) spectroscopy, have been employed to assess polymer-mediated electron transfer behaviour and the suitability of these nanocomposites for optoelectronic applications.

Structural and Chemical Characterization

The X-ray diffraction (XRD) analysis is an effective approach to investigate the crystallinity and interlayer spacing of the as-synthesized reduced graphene oxide. The XRD pattern of rGO and its composite with conducting polymer P3HT are shown in Figure 1(A).

The interlayer spacing information was evaluated on the basis of Bragg's law [34]:

$$\lambda=2d\sin(\theta) \quad (1)$$

where λ is the wavelength of the X-ray beam and usually taken as 0.154nm, d is the interlayer spacing of rGO, and θ is the diffraction angle.

$$d=\lambda/2\sin(\theta) \quad (2)$$

In addition, the rGO–P3HT nanocomposite was spin-coated on a glass substrate, and the average crystallite size of rGO domains within the composite was estimated using Scherrer's formula [35]:

$$\tau = K\lambda/\beta\cos(\theta) \quad (3)$$

As observed in Figure 1(A), the XRD pattern of reduced graphene oxide exhibits a broad diffraction peak centered at $2\theta \approx 25.95°$, corresponding to an interlayer spacing of approximately 0.327 nm. The characteristic diffraction peak of graphene oxide around $2\theta \approx 10°$ is absent after chemical reduction using L-glutathione, confirming the effective reduction of GO and partial restoration of graphitic ordering [32]. The XRD pattern of the rGO–P3HT nanocomposite does not show any additional sharp diffraction peaks compared to rGO. This indicates that incorporation of the conducting polymer does not significantly alter the crystalline structure of rGO and that P3HT remains largely amorphous within the composite matrix. The absence of distinct polymer-related diffraction features suggests homogeneous dispersion of rGO within the polymer matrix without inducing long-range crystallinity changes. These observations confirm the successful reduction of GO and the preservation of structural integrity, which are essential for facilitating efficient charge transport in the nanocomposite.

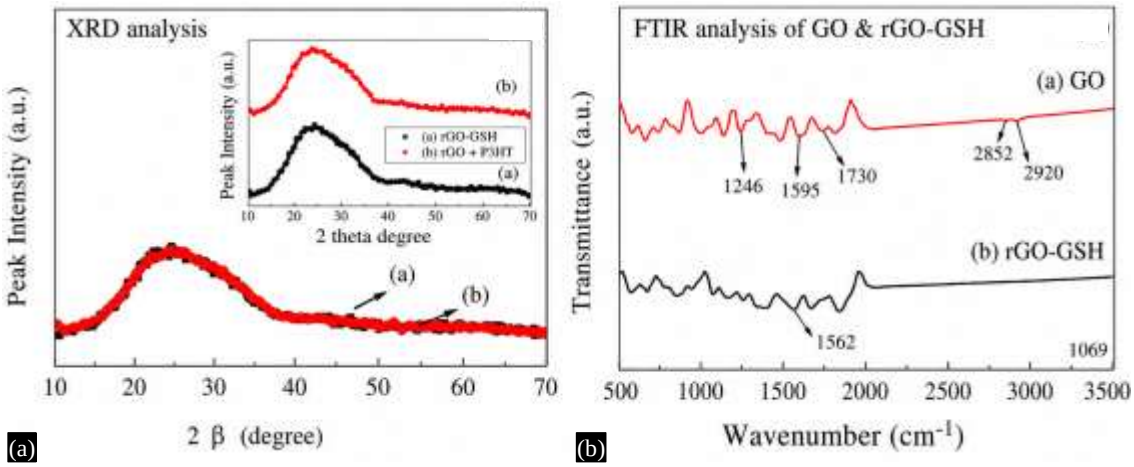

Figure 1. Structural and chemical characterization: (A) XRD Analysis of (a) reduced graphene oxide (rGO) (b) nanocomposite of rGO-P3HT, (B) FTIR spectra of GO and rGO(GSH) confirming reduction and functional group modification.

Further FT-IR spectroscopy was used to further explore the reduction of oxygen-containing functional groups and the nature of organic ligand coating on GO. The formation of the functional groups and bonding interactions of GO and polymer-compatible rGO(GSH) were examined using FTIR measurements in transmission mode in the region 4000-500 cm^{-1} as depicted in Figure 1(B). In the spectrum of GO, two small peaks at 2852 cm^{-1} and 2920 cm^{-1} are assigned to -CH_2 symmetric and asymmetric stretching vibrations, whereas the band present at 1730 cm^{-1} corresponds to C=O stretching associated with carboxylic groups. In addition, the absorption peak at 1595 cm^{-1} is attributed to the skeletal vibration of unoxidized graphitic domains, and another peak around 1246 cm^{-1} is assigned to C-O stretching vibrations arising from epoxy or alkoxy groups. These features collectively confirm the presence of oxygen-containing functional groups on GO sheets. However, in the spectrum of rGO(GSH), the intensity of peaks corresponding to oxygen-containing functional groups is significantly reduced, indicating successful chemical reduction.

The dominant peak observed at 1562 cm^{-1} corresponds to C=C skeletal vibrations of restored sp^2-hybridized carbon networks. The substantial attenuation of oxygen-related absorption bands confirms the effective removal of oxygen functionalities during reduction, while preserving the extended sp^2-conjugated graphitic domains, enabling interfacial interaction with the conducting polymer. The observed changes in functional groups further validate the effective reduction in GO and improved chemical compatibility between P3HT and rGO(GSH) nanocomposite.

Morphological Analysis

The surface morphology of reduced graphene oxide was examined using scanning electron microscopy (SEM), and images are depicted in Figure 2(A). The SEM micrographs reveal thin, sheet-like morphologies characteristic of exfoliated graphene-based material which remain stable under the electron beam. The observed morphology indicates the presence of few layered rGO sheets distributed over the glass substrate. The inset image further confirms the formation of overlapping and wrinkled rGO sheets, with lateral dimensions extending to hundreds of nanometers, which typical of chemically reduced GO prepared via solution-based routes.

Further insight into the surface topography where thickness of the GO and as-prepared rGO was investigated using atomic force microscopy (AFM). The typical AFM images were recorded in tapping mode to minimize tip-induced deformation and shown in Figure 2(B). The AFM image of GO exhibits relatively smooth sheet-like features with increased thickness due to the presence of oxygen-containing functional groups, whereas the rGO(GSH) sample shows reduced sheet thickness and increased surface corrugation, indicating effective removal of oxygen functionalities during chemical reduction.

The observed height profiles are consistent with few layer rGO sheets, confirming successful reduction while maintaining sheet integrity. Such morphological characteristics are favorable for uniform dispersion and effective interfacial contact within conducting polymer matrices. Such morphological features provide an increased interfacial area, which is favorable for enhanced polymer–rGO interaction and efficient charge transfer.

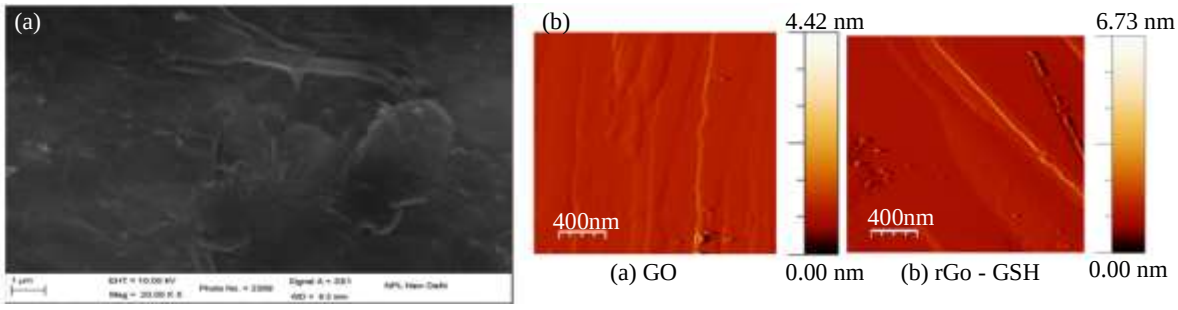

Figure 2. Morphological analysis of materials: (a) SEM image of rGO(GSH) showing sheet-like structure, (b) AFM image of GO, and rGO(GSH) indicating thickness reduction and surface corrugation after chemical reduction.

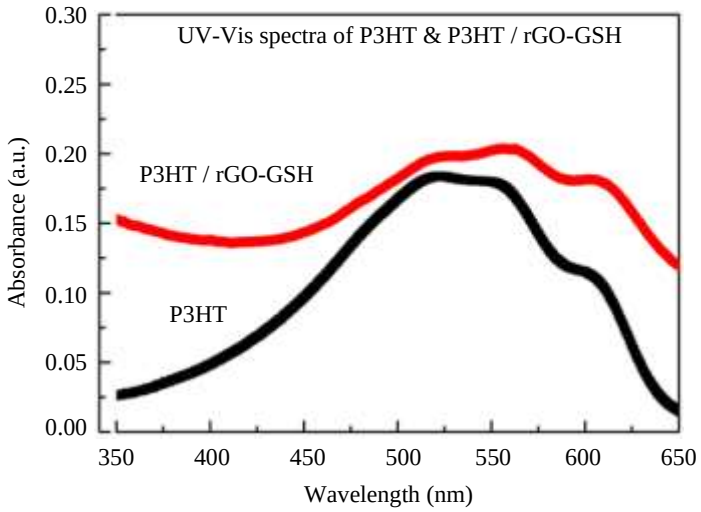

Figure 3. UV–Vis absorption spectra of pristine P3HT and P3HT/rGO(GSH) nanocomposites showing spectral broadening and red shift due to enhanced interfacial interaction.

Optical Absorption Studies

The absorption behaviour of pristine P3HT and their corresponding nanocomposites P3HT/rGO(GSH) is shown in Figure 3. The absorption spectra of GO and rGO(GSH) exhibit gradually varying absorption profiles, providing characteristics of graphene-based material. Whereas, the spectrum of rGO(GSH) shows a less steep absorption edge compared to GO, indicating partial restoration of π-conjugation following chemical reduction [34]. The absorption spectrum of pristine P3HT reveal a wide absorption band cantered around 530 nm, which can be attributed to the π-π* transition of the conjugated polymer backbone [36]. Upon incorporation of rGO(GSH), the absorption spectrum of P3HT-rGO(GSH) nanocomposites become broader, with a slight red shift, suggesting enhanced electronic interaction at the polymer-rGO interface. This spectral broadening indicates improved light-harvesting capability over a wider wavelength range. The observed changes in the absorption characteristics can be attributed to polymer-mediated electronic interactions, where the presence of rGO(GSH) influences the effective conjugation length and excitonic behavior of P3HT chains. The contribution of eco-friendly reduced graphene oxide as an interfacial acceptor enhances absorption intensity in the composite, supporting its suitability for optoelectronic and light-harvesting applications. This behaviour indicates enhanced interfacial interaction and improved light-harvesting capability, which are crucial for optoelectronic applications.

To understand the whole framework of polymer-mediated electron transfer in the P3HT–rGO(GSH) nanocomposite system, a schematic representation is illustrated in Figure 4. Upon photoexcitation, excitons (electron–hole pairs) are generated within the conjugated polymer (P3HT) matrix and favourable interfacial interaction between P3HT and rGO(GSH) takes place. Subsequently, these excitons undergo efficient dissociation at the donor-acceptor (P3HT–rGO) interface. The presence of rGO(GSH) as an electron acceptor material facilitates the transfer of photogenerated electrons from the excited state of P3HT, while holes remain on the polymer backbone, leading to effective charge separation. This process is further supported by π–π interactions between the conjugated polymer chains in P3HT and the sp^2-hybridized carbon network of rGO(GSH), which further enhances interfacial electronic coupling. As a result, radiative recombination is suppressed which leads to effective charge separation and improves electron transport within the nanocomposite system.

Photoluminescence Studies

The photoluminescence (PL) based spectroscopic investigation was carried out to study polymer-mediated excited-state electron transfer in nanocomposites consisting of the conducting donor polymer P3HT and rGO(GSH) as the acceptor material. The PL spectra were recorded at an excitation

wavelength (λ_{excit}) of 450 nm and the corresponding emission maximum (λ_{max}) was observed at 582 nm, shown in Figure 5. The quenching of photoluminescence intensity upon the incorporation of rGO(GSH) is attributed to the ability of rGO(GSH) to act as an efficient electron acceptor, thereby reducing the relative recombination of excitons generated with in the polymer matrix. It is worth mentioning that the gradual addition of rGO(GSH) in varying concentrations, a systematic decrease in the PL intensity of P3HT is observed, indicating efficient excited-state electron transfer from P3HT to rGO(GSH) at the polymer–acceptor interface.

The observed PL quenching behaviour suggests enhanced interfacial electronic coupling between P3HT chains and rGO(GSH), facilitated by π-π^* interactions between the conjugated polymer backbone and the sp^2-hybridized carbon network of rGO. However, the reduction in emission intensity is primarily associated with non-radiative decay pathways induced by electron transfer rather than energy transfer, as no significant spectral overlap between the absorption spectrum of rGO(GSH) and the emission spectrum of P3HT is observed. This noticeable quenching behaviour strongly confirms the efficient electron transfer from P3HT to rGO(GSH), supporting the proposed polymer-mediated charge transfer Mechanism.

Stern–Volmer Analysis

To quantitatively understand the mechanism of Pl quenching in the conducting polymer–based nanocomposite P3HT/rGO(GSH), Stern-Volmer (SV) model was employed. According to Stern-Volmer theory [37], the quenching behaviour can be expressed as –

$$F_0 / F_x = 1 + K_{SV}[Q] \quad (4)$$

where F_0 and F_x represent the fluorescence intensities of P3HT in the absence and presence of rGO(GSH), respectively, K_{SV} is the Stern–Volmer quenching constant, and Q denotes the concentration of rGO(GSH) acting as the quencher.

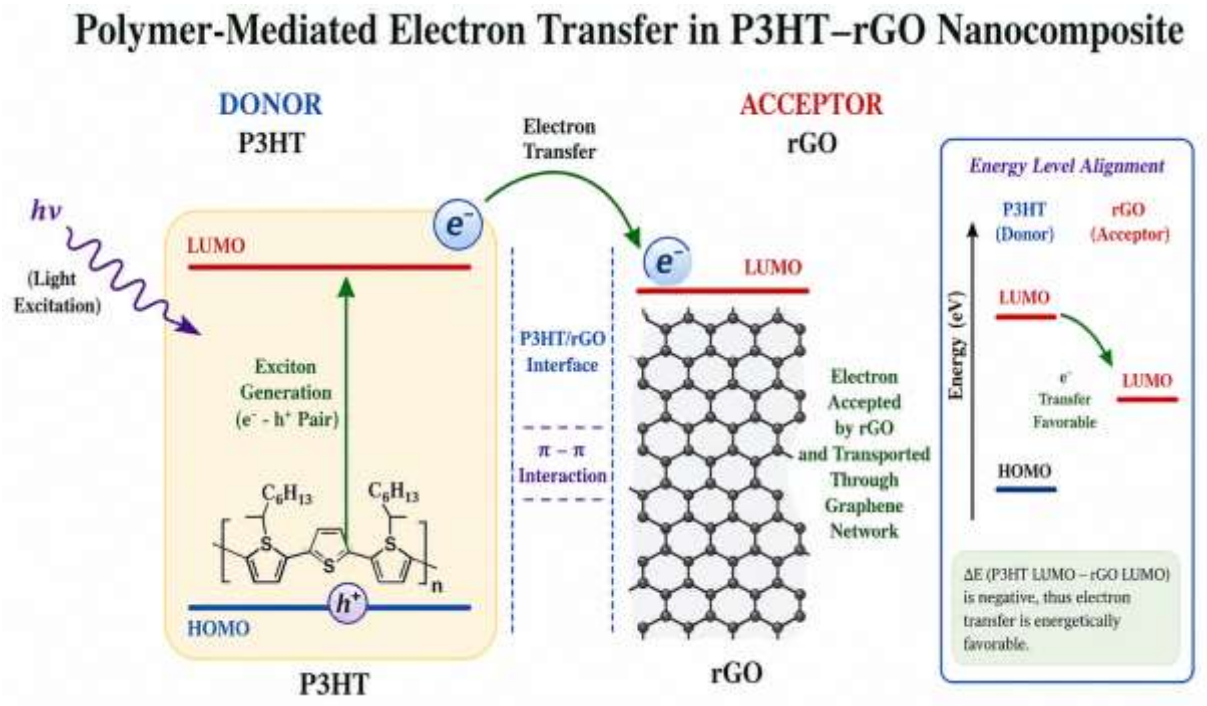

Figure 4. Schematic illustration of polymer-mediated electron transfer mechanism in P3HT–rGO nanocomposite under photoexcitation.

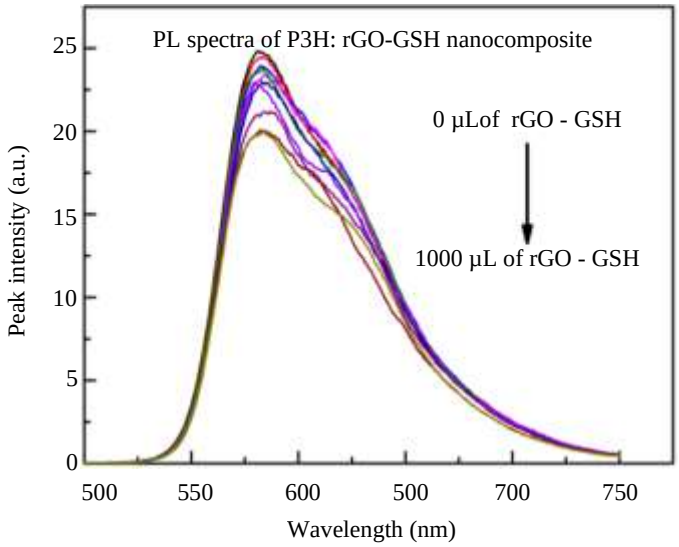

Figure 5. Photoluminescence spectra of P3HT and P3HT/rGO(GSH) nanocomposites showing systematic quenching indicating efficient electron transfer.

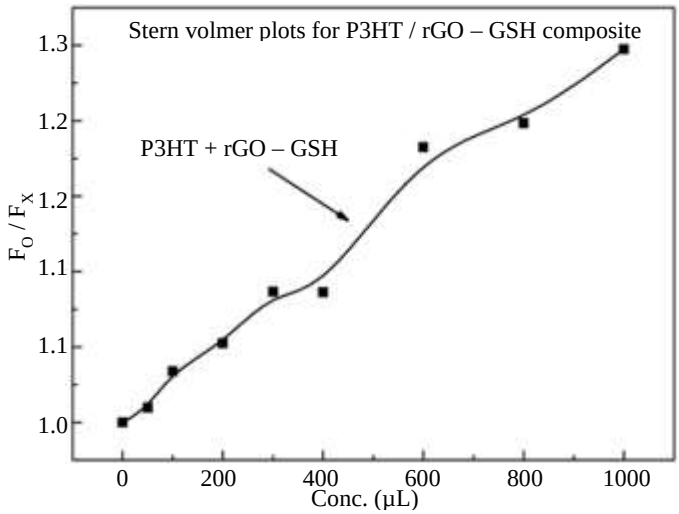

Figure 6. Stern–Volmer plot for P3HT/rGO(GSH) nanocomposite showing linear quenching behavior at lower concentrations and deviation at higher concentrations.

According to Stern–Volmer theory, a plot of F_0/F_x (fluorescence intensity ratio) versus Q (quencher concentration) is expected to exhibit linear behavior under conditions dominated by dynamic quenching, with slope corresponding to the Stern-Volmer quenching constant (K_{SV}) [38]. Figure 6, shows the Stern–Volmer plot for P3HT/rGO(GSH) nanocomposite, from which a K_{SV} value of 1.24×10^3 L^{-1} was extracted. At lower concentrations of rGO(GSH), the SV plot exhibits a linear relationship, indicating that a dynamic quenching dominated by excited-state electron transfer is the primary mechanism. At higher quencher concentrations, a slight deviation from linearity is observed, which may arise from static quenching effects or limited accessibility of polymer excitons to additional rGO sheets, such situations are still ambiguous. At increased rGO(GSH) concentrations, partial aggregation or overlapping of rGO sheets due to van der Waals interactions may occur, leading to the formation of multilayer rGO domains. Such structural arrangements can enhance quenching efficiency by increasing the effective interfacial area between the polymer donor and rGO acceptor, resulting in the observed nonlinearity in the SV plot [39]. Importantly, the absence of significant spectral overlap between the absorption spectrum of rGO(GSH) and the emission spectrum of P3HT confirms that the quenching process is governed predominantly by electron transfer rather than Förster-type energy transfer mechanisms. This observation further substantiates efficient polymer-mediated excited-state electron

transfer at the P3HT–rGO(GSH) interface. The observed quenching behavior further substantiates the existence of strong interfacial interactions and efficient charge transfer dynamics within the nanocomposite system.

CONCLUSIONS

The present work demonstrates an eco-friendly approach for the reduction of GO and its effective integration with a conducting polymer matrix (P3HT) for optoelectronic applications. The successful reduction of graphene oxide using L-glutathione as a green reducing agent was confirmed through comprehensive spectroscopic and structural characterization techniques. Furthermore, homogeneous nanocomposites of conducting polymer P3HT and rGO(GSH) were prepared using a simple solution-processing method and systematically investigated. Spectroscopic studies, including UV–Vis absorption and photoluminescence analysis, revealed significant quenching behavior, which was further supported by Stern–Volmer analysis, confirming efficient polymer-mediated electron transfer at the donor–acceptor interface. Overall, the obtained results emphasize that interfacial engineering in the P3HT–rGO(GSH) hybrid nanocomposite plays a more critical role than simple material incorporation in enhancing electron transfer efficiency. This establishes a clear relationship between structural compatibility and charge transfer dynamics, providing a strong foundation for the design of eco-friendly and high-performance nanocomposites for optoelectronic applications.

Acknowledgments

Sumit Kumar gratefully acknowledges Dr Chenraj Roychand, Chancellor, JAIN (Deemed-to-be University) Bangalore, India for continuous administrative and institutional support. Tanvi Vats, Ashu Soni, and Pratibha Tiwari acknowledge their respective affiliations with Gautam Buddha University, Greater Noida; Bharati Vidyapeeth College of Engineering, New Delhi; and Hansraj College, University of Delhi, during the course of this work.

Author Contributions

Sumit Kumar conceived the research idea, designed the overall study, carried out the experimental work as an extension of previously published work [34], and led the data interpretation. He also prepared the original draft of the manuscript and coordinated all revisions. Tanvi Vats, Ashu Soni and Pratibha Tiwari contributed to the interpretation of results and provided critical inputs during manuscript refinement. All authors reviewed, discussed, and approved the final version of the manuscript.

Conflicts of Interest

The authors declare that there are no conflicts of interest. This article does not contain any studies involving human or animal subjects.

REFERENCES

1. Shankar U, Sethi SK, Singh BP, Kumar A, Manik G, Bandyopadhyay. A Optically transparent and lightweight nanocomposite substrate of poly (methyl methacrylate-co-acrylonitrile)/MWCNT for optoelectronic applications: an experimental and theoretical insight. Journal of Materials Science. 2021; 56(30):17040–61.
2. Nguyen. TP Polymer-based nanocomposites for organic optoelectronic devices. A review. Surface and Coatings Technology. 2011; 206(4):742–52.
3. Sagadevan S, Shahid MM, Yiqiang Z, Oh WC, Soga T, Anita Lett J, Alshahateet SF, Fatimah I, Waqar A, Paiman S, Johan. MR Functionalized graphene-based nanocomposites for smart optoelectronic applications. Nanotechnology Reviews. 202;10(1):605–35.
4. Norrman. K Stability and Degradation of Polymer Solar cells. In3rd International Summit on OPV Stability. 2010.

5. Feng L, Chen M, Zheng F, Niu MS, Zhang X, Hao. XT Efficient photoinduced charge transfer in chemically-linked organic-metal Ag-P3HT nanocomposites. Optical Materials Express. 2016; 6(10):3063–74.
6. V Molefe F, Khenfouch M, S Dhlamini M, M Mothudi. B Spectroscopic investigation of charge and energy transfer in P3HT/GO nanocomposite for solar cell applications. Advanced Materials Letters. 2017; 8(3):246–50.
7. Geim AK, Novoselov. KS The rise of graphene. Nature materials. 2007; 6(3):183-91.
8. Lee C, Wei X, Kysar JW, Hone. J Measurement of the elastic properties and intrinsic strength of monolayer graphene. science. 2008; 321(5887):385–8.
9. Bolotin KI, Sikes KJ, Jiang Z, Klima M, Fudenberg G, Hone J, Kim P, Stormer. HL Ultrahigh electron mobility in suspended graphene. Solid state communications. 2008; 146(9-10):351–5.
10. Garg R, Elmas S, Nann T, Andersson. MR Deposition methods of graphene as electrode material for organic solar cells. Adv Energy Mater 2017; 7(10):1601393.
11. Xu M, Qi J, Li F, Liao X, Liu S, Zhang. Y Ultra-thin, transparent and flexible tactile sensors based on graphene films with excellent anti-interference. RSC advances. 2017;7(48):30506–12.
12. Thompson BC, Murray E, Wallace. GG Graphite oxide to graphene. Biomaterials to bionics. Advanced Materials. 2015; 27(46):7563–82.
13. Shuai X, Bo Z, Kong J, Yan J, Cen. K Wettability of vertically-oriented graphenes with different intersheet distances. RSC Advances. 2017;7(5):2667–75.
14. Tang C, Li BQ, Zhang Q, Zhu L, Wang HF, Shi JL, Wei. F CaO-templated growth of hierarchical porous graphene for high-power lithium–sulfur battery applications. Advanced Functional Materials. 2016; 26(4):577–85.
15. Tarcan R, Todor-Boer O, Petrovai I, Leordean C, Astilean S, Botiz. I Reduced graphene oxide today. Journal of Materials Chemistry C. 2020;8(4):1198–224.
16. Marta B, Leordean C, Istvan T, Botiz I, Astilean. S Efficient etching-free transfer of high quality, large-area CVD grown graphene onto polyvinyl alcohol films. Applied Surface Science. 2016; 363:613–8.
17. Su CY, Lu AY, Xu Y, Chen FR, Khlobystov AN, Li. LJ High-quality thin graphene films from fast electrochemical exfoliation. ACS nano. 2011; 5(3):2332–9.
18. Cao J, He P, Mohammed MA, Zhao X, Young RJ, Derby B, Kinloch IA, Dryfe. RA Two-step electrochemical intercalation and oxidation of graphite for the mass production of graphene oxide. Journal of the American Chemical Society. 2017; 139(48):17446–56.
19. Liu B, Xie J, Ma H, Zhang X, Pan Y, Lv J, Ge H, Ren N, Su H, Xie X, Huang. L From graphite to graphene oxide and graphene oxide quantum dots. Small. 2017; 13(18):1601001.
20. Agresti A, Pescetelli S, Cinà L, Konios D, Kakavelakis G, Kymakis E, Carlo. AD Efficiency and stability enhancement in perovskite solar cells by inserting lithium-neutralized graphene oxide as electron transporting layer. Advanced Functional Materials. 2016 ;26(16):2686–94.
21. Liu J, Xu M, Wang B, Zhou Z, Wang. L Fluorescence sensor for detecting protamines based on competitive interactions of polyacrylic acid modified with sodium 4-amino-1-naphthalenesulfonate with protamines and aminated graphene oxide. RSC advances. 2017; 7(3):1432–8.
22. Li Z, Gadipelli S, Yang Y, Guo. Z Design of 3D graphene-oxide spheres and their derived hierarchical porous structures for high performance supercapacitors. Small. 2017; 13(44):1702474.
23. Zhang M, Zhou N, Yuan P, Su Y, Shao M, Chi. C Graphene oxide and adenosine triphosphate as a source for functionalized carbon dots with applications in pH-triggered drug delivery and cell imaging. RSC advances. 2017; 7(15):9284–93.
24. Kang KM, Kim DW, Ren CE, Cho KM, Kim SJ, Choi JH, Nam YT, Gogotsi Y, Jung. HT Selective molecular separation on Ti3C2T x–graphene oxide membranes during pressure-driven filtration: comparison with graphene oxide and MXenes. ACS applied materials & interfaces. 2017; 9(51):44687–94.
25. Zaharie-Butucel D, Potara M, Craciun AM, Boukherroub R, Szunerits S, Astilean. S Revealing the structure and functionality of graphene oxide and reduced graphene oxide/pyrene carboxylic acid

interfaces by correlative spectral and imaging analysis. Physical Chemistry Chemical Physics. 2017;19(24):16038–46.
26. Sharma M, Sharma N, Alvi PA, Gupta SK, Negi CM. P3HT-rGO composites for high-performance optoelectronic devices. Optical Materials. 2022 May 1; 127:112326.
27. Xiao X, Zhang Y, Zhou L, Li B, Gu. L Photoluminescence and fluorescence quenching of graphene oxide: a review. Nanomaterials. 2022; 12(14):2444.
28. Iliut M, Leordean C, Canpean V, Teodorescu CM, Astilean. S A new green, ascorbic acid-assisted method for versatile synthesis of Au–graphene hybrids as efficient surface-enhanced Raman scattering platforms. Journal of Materials Chemistry C. 2013;1(26):4094–104.
29. Zhan D, Ni Z, Chen W, Sun L, Luo Z, Lai L, Yu T, Wee AT, Shen. Z Electronic structure of graphite oxide and thermally reduced graphite oxide. Carbon. 2011; 49(4):1362–6.
30. Iskandar F, Hikmah U, Stavila E, Aimon. AH Microwave-assisted reduction method under nitrogen atmosphere for synthesis and electrical conductivity improvement of reduced graphene oxide (rGO). RSC advances. 2017; 7(83):52391–7.
31. Gao W, Alemany LB, Ci L, Ajayan. PM New insights into the structure and reduction of graphite oxide. Nature chemistry. 2009; 1(5):403–8.
32. Pham TA, Kim JS, Kim JS, Jeong. YT One-step reduction of graphene oxide with L-glutathione. Colloids and Surfaces A: Physicochemical and Engineering Aspects. 2011 ;384(1-3):543–8.
33. Chua CK, Pumera. M Chemical reduction of graphene oxide: a synthetic chemistry viewpoint. Chemical Society Reviews. 2014; 43(1):291–312.
34. Kumar S, Kumar J, Sharma SN, Srivastava. S. rGO integrated MEHPPV and P3HT polymer blends for bulk hetero junction solar cells: a comparative insight. Optik. 2019; 178:411–21.
35. Kumar S, Sharma SN, Kumar. J Comparative charge transport study of MEHPPV–TiO2 and P3HT–TiO2 nanocomposites for hybrid bulk heterojunction solar cells. Journal of Nanoscience and Nanotechnology. 2019; 19(6):3408–19.
36. Shrotriya V, Ouyang J, Tseng RJ, Li G, Yang. Y Absorption spectra modification in poly (3-hexylthiophene): methanofullerene blend thin films. Chemical physics letters. 2005; 411(1–3):138–43.
37. Albrecht C. Joseph R. Lakowicz: *Principles of fluorescence spectroscopy*, 3rd edition. *Analytical and Bioanalytical Chemistry.* 2008; 390:1223–1224. doi: 10.1007/s00216-007-1843-5.
38. Kumar S, Kumar J, Sharma. SN Investigation of charge transfer properties in MEHPVV and rGO-AA nanocomposites for Green organic photovoltaic application. Optik. 2020; 208:164540.
39. Das S, Wajid AS, Shelburne JL, Liao YC, Green. MJ Localized in situ polymerization on graphene surfaces for stabilized graphene dispersions. ACS applied materials & interfaces. 2011; 3(6):1844–51.

